

# The fabrication of x-ray masks using proton beam writing

Weisheng Yue<sup>1</sup>, Sher-Yi Chiam<sup>1</sup>, Yaping Ren<sup>2</sup>, Jeroen Anton van Kan<sup>1</sup>,  
Thomas Osipowicz<sup>1</sup>, Linke Jian<sup>2</sup>, Herbert O Moser<sup>2</sup> and Frank Watt<sup>1</sup>

<sup>1</sup> Centre for Ion Beam Applications, Department of Physics, National University of Singapore, Singapore 117542, Singapore

<sup>2</sup> Singapore Synchrotron Light Source, National University of Singapore, 5 Research Link, Singapore 117603, Singapore

E-mail: [phyto@nus.edu.sg](mailto:phyto@nus.edu.sg) (Thomas Osipowicz)

Received 3 April 2008, in final form 25 May 2008

Published 4 July 2008

Online at [stacks.iop.org/JMM/18/085010](http://stacks.iop.org/JMM/18/085010)

## Abstract

We have developed a simplified method of fabricating x-ray masks for deep x-ray lithography by using proton beam writing (PBW) without subsequent soft x-ray copying steps. Combining direct PBW and subsequent electroplating, x-ray masks with gold absorber patterns of up to 11  $\mu\text{m}$  height and with vertical and smooth sidewalls were fabricated. The smallest size in the absorber pattern is less than 0.5  $\mu\text{m}$  in this work. The masks were used for x-ray lithography with synchrotron radiation, and 870  $\mu\text{m}$  SU-8 structures with smooth sidewalls were produced. This fabrication method is promising to be an important alternative to conventional methods for x-ray mask making.

(Some figures in this article are in colour only in the electronic version)

## 1. Introduction

The LIGA (a German acronym for lithography, electroplating and molding) process is an important technology for the production of high aspect ratio micro- and nanostructures [1, 2]. The technological core of LIGA is x-ray lithography with synchrotron radiation (SR). In this process, absorber patterns in a mask are transferred to a resist layer and in the case of positive (negative) resist, a suitable developer dissolves the irradiated (non-irradiated) zones within this resist layer. The properties of the x-ray mask limit the accuracy and the achievable aspect ratio of the resulting microstructures, and therefore the fabrication of the x-ray mask is one of the most important and critical steps in the LIGA process [3]. An x-ray mask should simultaneously have sufficient absorber thickness and display sub-micrometer features. Clearly, these requirements present a challenge for sub-micrometer x-ray mask fabrication. Electron beam lithography is one of the most widely used direct writing techniques for x-ray mask fabrication. However, e-beam lithography is typically performed on relatively thin resist layers (less than 1  $\mu\text{m}$ ), which do not provide sufficient contrast for hard x-ray lithography [2]. To make a sufficiently

thick absorber layer (say 10–20  $\mu\text{m}$ ), conventional x-ray mask production has to use several lithography steps in two or more exposures [4]. First, an intermediate mask with a high resolution pattern is produced by electron beam writing or other direct writing techniques. In the case of electron beam writing, the thickness of the patterned layer is usually about 1  $\mu\text{m}$ . After electroplating, the pattern in the intermediate mask is transferred to a thicker resist using soft x-ray lithography. The patterns in the resist are then plated with gold to form the final working mask, which is then used for deep x-ray lithography with SR to produce high-quality structures. Due to the large number of process steps when the intermediate mask copy is involved, the quality of the final mask may be negatively influenced with respect to pattern transfer accuracy and electron beam proximity effects, for example. Other methods, e.g. the use of anodized aluminum oxide pores as x-ray masks, were reported by Knaack *et al* [5], but this method cannot produce arbitrarily designed patterns. Therefore, a direct writing method without an intermediate mask step for x-ray mask fabrication would be highly advantageous.

Proton beam writing (PBW) is a high-potential direct writing technique capable of patterning 3D high aspect ratio structures with feature sizes down to the 20 nm level, a

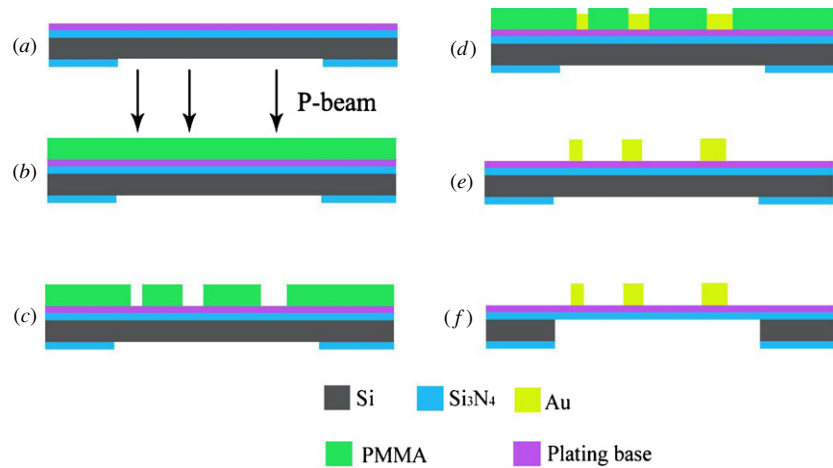


**Figure 1.** Schematic of the process of x-ray mask fabrication. (a) Coating conductive layers (Au 40 nm/Cr 10 nm) onto the front surface of the  $\text{Si}_3\text{N}_4$  membrane, (b) PMMA coating and proton beam writing, (c) development of PMMA patterns, (d) Au electroplating of the PMMA mold, (e) PMMA stripping and (f) backside silicon etching.

smoothness of less than 3 nm and large aspect ratios ( $\sim 160$ ) [6, 7]. A focused proton beam of several MeV energy is scanned in a predetermined pattern over a suitable resist (e.g., PMMA, SU-8 or HSQ), which is subsequently chemically developed. The technique of PBW is similar to that of electron beam lithography. Unlike electron beams, the small lateral straggling and minimal proximity effects of the proton beam result in high aspect ratio 3D structures with vertical sidewalls and sharp edges [8]. A high energy proton beam can penetrate very deep into resist in a very straight path. For example, a 2 MeV proton beam can penetrate more than  $60 \mu\text{m}$  into the PMMA resist. This is a particular advantage for x-ray mask making because it allows us to fabricate a very thick absorber layer. PBW thus is ideally suitable for the fabrication of x-ray masks. X-ray lithography then allows the pattern to be duplicated multiple times in much thicker resist than can be achieved with PBW. These advantages of the x-ray mask making, using MeV proton beam lithography, have been realized more than 10 years ago [9]. Recently, van Kan *et al* demonstrated the possibility of x-ray mask fabrication using proton beam writing and presented some preliminary experimental results [10]. However, an applicable x-ray mask has not been fabricated by using PBW yet. This work is aimed to develop a direct writing method without an intermediate mask step for x-ray mask fabrication by utilizing PBW.

## 2. Experiments

### 2.1. The x-ray mask fabrication process

Gold was selected as material for the absorber layer in our work. This is because Au has excellent physicochemical stability and can absorb x-rays efficiently due to its high atomic number. The Au absorber layer is fabricated on a  $1 \mu\text{m}$  thick  $\text{Si}_3\text{N}_4$  membrane supported by a silicon frame.  $\text{Si}_3\text{N}_4$  is highly transparent to x-rays and has sufficient mechanical strength to support the Au absorber structures because of its low-Z and good mechanical properties. The fabrication process is schematically shown in figure 1. The  $\text{Si}_3\text{N}_4$  membrane was

coated on both sides of the silicon wafer. The substrates were purchased (from Silson Pte Ltd, UK) as unetched wafers (with the Si backing behind the  $\text{Si}_3\text{N}_4$  windows intact). The front side of the silicon nitride was coated with a 10 nm Cr layer and then a 40 nm Au layer with magnetron sputtering. The gold layer serves as the seed layer for gold electroplating and Cr serves as an adhesion layer. Then, the substrates were spin-coated with the PMMA resist (950k A11 from MicroChem Pte Ltd) to a thickness of about  $15 \mu\text{m}$ . PBW experiments for this work were performed at the Centre for Ion Beam Applications (CIBA), National University of Singapore, using a focused beam of 2 MeV protons. Details of this facility have been reported elsewhere [11]. We fabricated gold structures that range in size from  $0.4 \mu\text{m}$  to  $20 \mu\text{m}$ .

A G-G developer was used to develop PMMA patterns. The G-G developer is a mixture of 60 vol% butoxyethoxyethanol, 20 vol% tetrahydro-oxazine, 15 vol% water and 5 vol% aminoethanol [12]. The sample was developed for up to 40 min at a temperature of  $20^\circ\text{C}$ . After development, the sample was rinsed with DI water. In this work, we found that the combination of the G-G developer and low temperature helps to improve the sidewall quality of thick gold structures. A gold electrolyte solution MICROFAB Au 100 was used for electroplating. During the process, the temperature of the water heat bath was kept at  $60^\circ\text{C}$  and the plating current density was set at a constant value of  $2.5 \text{ mA cm}^{-2}$ . A magnetic stirrer was used to provide agitation throughout the plating process which improved uniformity of the solution. The deposition speed was about  $1 \mu\text{m}$  of plated Au in every 5 min. When a sufficient thickness of Au had been deposited, the PMMA around the gold structures was removed by immersion in toluene at  $40^\circ\text{C}$ . The final step is backside Si wet etching with a concentrated KOH (30% by weight) solution at  $80^\circ\text{C}$ . The etching step usually takes several hours. After the etching, we have a complete mask consisting of Au absorber patterns supported by a  $\text{Si}_3\text{N}_4$  window in a Si frame. An x-ray mask is schematically illustrated in figure 2: there is a gold frame on the edge of the square  $\text{Si}_3\text{N}_4$  window and small gold patterns are in the center of the  $\text{Si}_3\text{N}_4$  window. The large gold

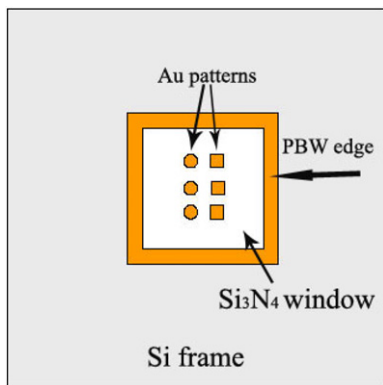


**Figure 2.** Schematic illustration of an x-ray mask. Au patterns are reproduced on the  $\text{Si}_3\text{N}_4$  membrane.

frame was fabricated using conventional UV lithography and served as a dummy area for the electroplating process. One edge of the frame (indicated by an arrow) was smoothed by cutting back the PMMA resist with PBW. The other edges were produced with simple masked UV lithography. The PBW edge is expected to produce a smooth SU-8 sidewall after x-

ray lithography, on which atomic force microscopy (AFM) measurement takes place.

### 2.2. X-ray exposure

Test x-ray exposures were done to evaluate the quality of x-ray masks. The experiments were carried out at the Lithography for Micro- and NanoTechnology (LiMiNT) beamline of Singapore Synchrotron Light Source (SSLS) [13]. With an electron energy of 700 MeV and a magnetic flux density of 4.5 T, the critical photon energy of the Helios 2 storage ring is 1.47 keV. The photon beam passes through two Be windows, each  $200\ \mu\text{m}$  thick, and about 80 cm of gaseous He at a pressure of 100 mbar at room temperature. Upstream the mask, the photon spectrum peaks at about 4.5 keV and decreases to 10% of the maximum at 2.5 and 10 keV. At an electron current of 300 mA, the maximum photon flux density at the mask is  $6 \times 10^{11}$  photons/(s · mrad<sup>2</sup> · 0.1% rbw). SU-8 resist was used for the exposure. A  $13\ \mu\text{m}$  thick Kapton filter was placed between the mask and the SU-8 resist layer. For the  $870\ \mu\text{m}$  thick SU-8 resist, the exposure time was 7 min. The x-ray scanner chamber was filled with gaseous He of a pressure of 100 mbar at room temperature. The x-ray scanner together

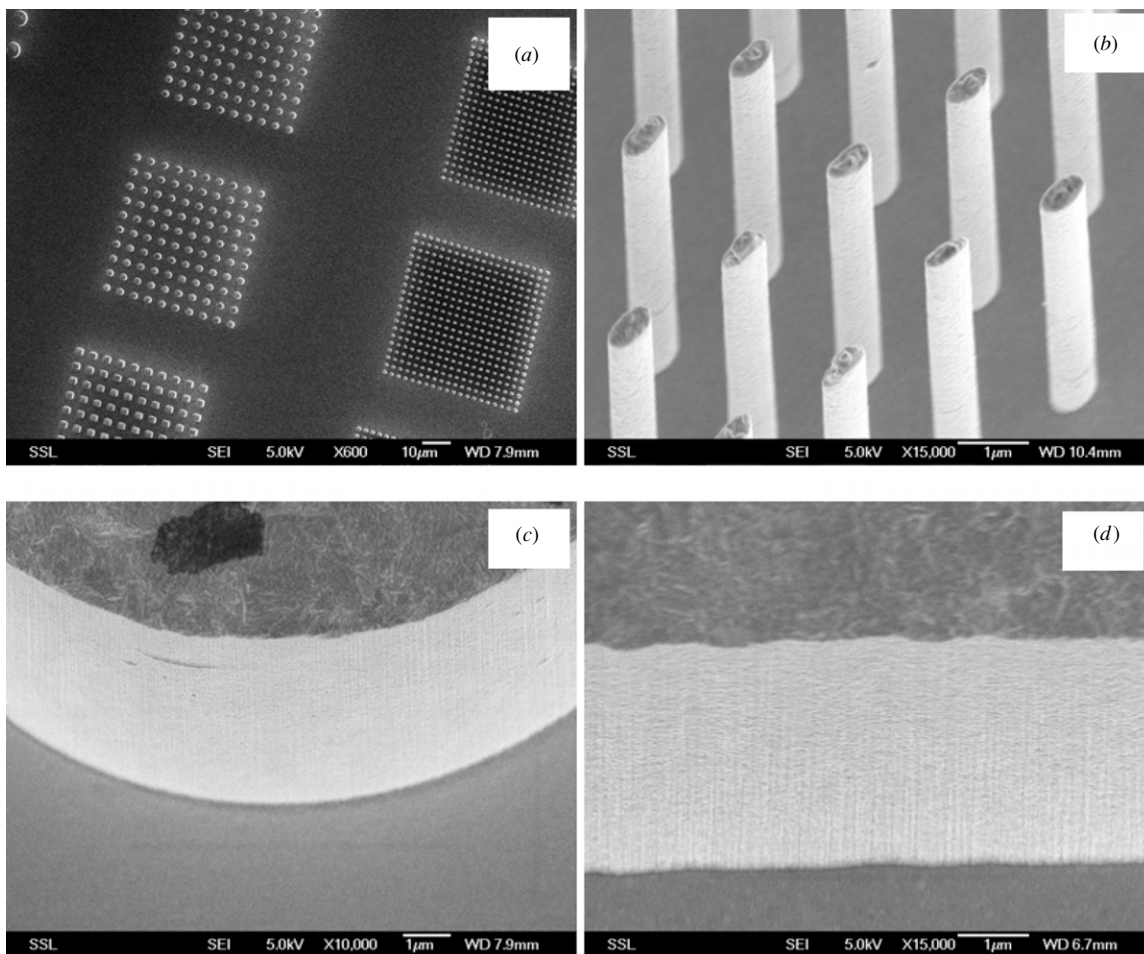


**Figure 3.** SEM images of Au patterns fabricated with PBW. (a) Top view of some gold pillars, (b) Au pillars with a  $0.4\ \mu\text{m}$  size of  $9.5\ \mu\text{m}$  height, (c) close view of a  $20\ \mu\text{m}$  diameter pillar with a height of  $10.7\ \mu\text{m}$ , (d) close view of a  $20\ \mu\text{m}$  size square pillar with a height of  $10.4\ \mu\text{m}$ .

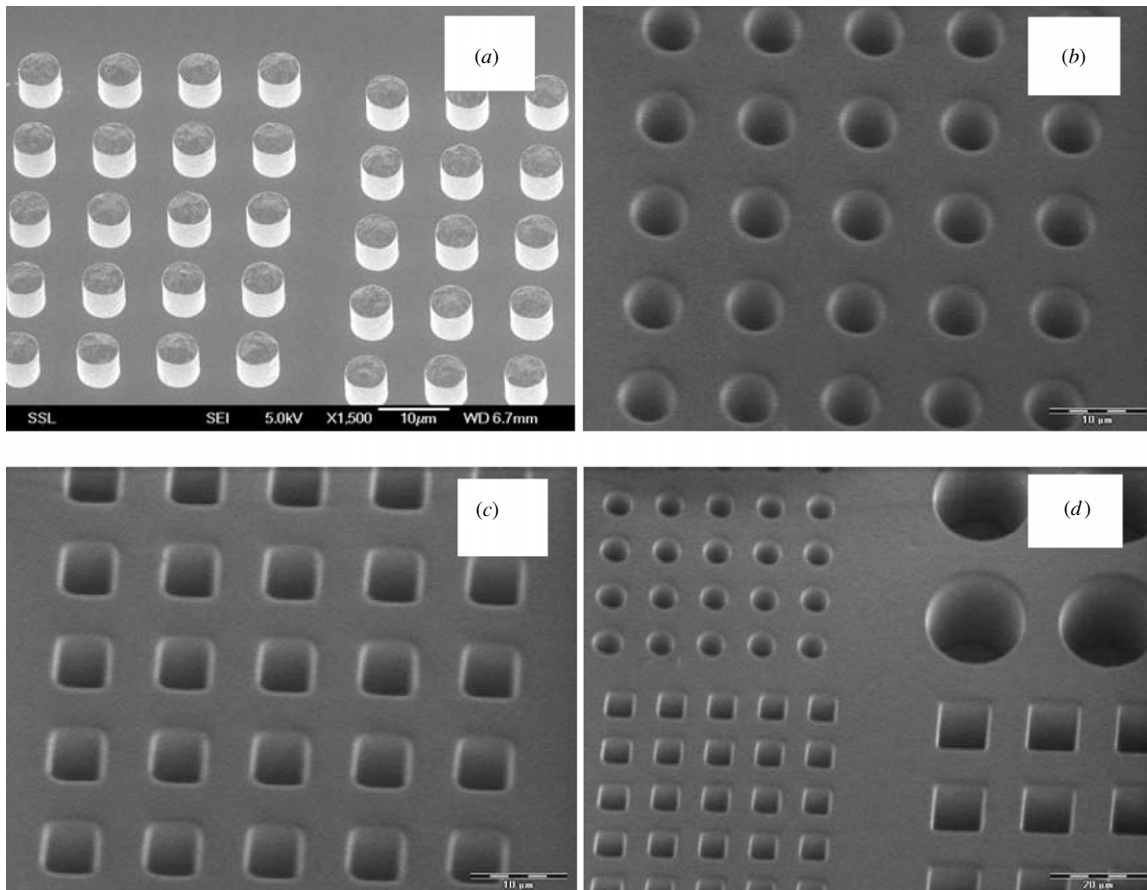


**Figure 4.** (a) SEM images of gold pillars on an x-ray mask, (b) SU-8 circular holes produced by x-ray exposure of patterns in (a), (c) SU-8 square holes, (d) an overview of SU-8 microstructures with different shapes.

with the whole LIGA process equipment is located in a class 1000 clean room at SSLs.

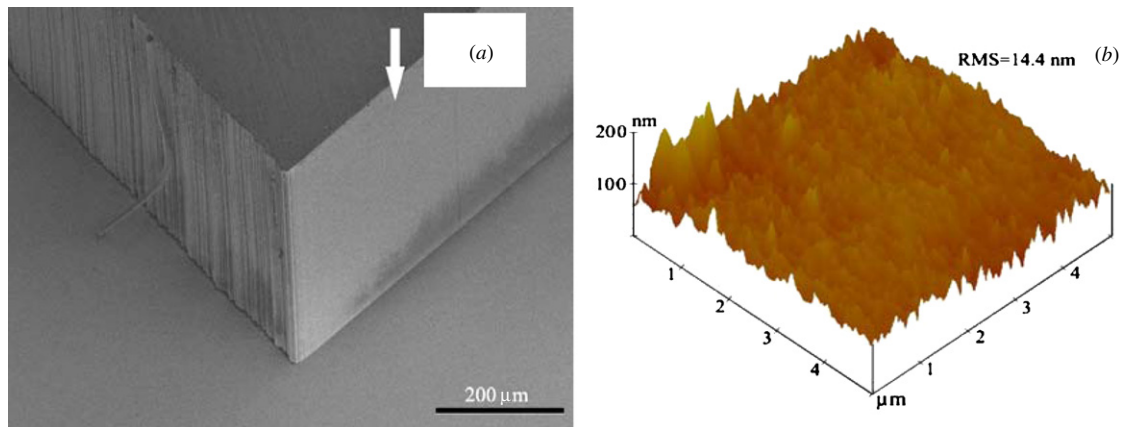
### 3. Results and discussion

Figure 3 shows some of Au patterns fabricated with PBW. Figure 3(a) is a top view of patterns on the  $\text{Si}_3\text{N}_4$  membrane and figure 3(b) shows a close view of small pillars. The size of pillars in figure 3(b) is  $0.4\ \mu\text{m}$  and the height is  $9.5\ \mu\text{m}$ , giving an aspect ratio of 23. We note that the aspect ratios of these Au pillars are, to our knowledge, the largest ones as yet produced by direct writing techniques. As mentioned previously, the most significant feature of PBW is that it can produce very tall structures with vertical and smooth sidewalls down to the 20 nm level. Sidewall images are shown in figures 3(c) and (d). Figure 3(c) is a close view of the sidewall of a  $20\ \mu\text{m}$  diameter circular pillar and figure 3(d) is the sidewall of a  $20\ \mu\text{m}$  size square pillar. Their heights are  $10.7\ \mu\text{m}$  and  $10.4\ \mu\text{m}$  respectively. Au absorbers of such thickness are well suited for x-ray lithography. By visual inspection, the sidewall is very vertical. Quantitatively, the verticality of sidewalls was calculated with the methods reported by van Kan *et al* [14], and found that the deviation from  $90^\circ$  is less than  $0.4^\circ$ .

The thickness of absorbers in our masks was more than  $10\ \mu\text{m}$ . Absorption contrast (commonly referred to as

contrast) is commonly used to evaluate the suitability of an x-ray mask for patterning a given thickness resist layer. The contrast  $c$  is defined as the ratio of the bottom dose  $d_B$  to the top dose  $d_T$  under the absorber, namely  $c = d_B/d_T$  [2]. Calculations with the DoseSim code, which allows us to simulate the exposure features of x-ray lithography [15], indicate that the masks with a  $10.7\ \mu\text{m}$  absorber provide a contrast of 77, for the  $870\ \mu\text{m}$  thick SU-8 layers. Figure 4(a) shows an SEM image of Au pillars on a  $\text{Si}_3\text{N}_4$  membrane and figure 4(b) shows the corresponding SU-8 patterns that were produced by x-ray exposure of the Au pillars in deep x-ray lithography. It shows that the patterns were fairly well duplicated by x-ray lithography. Figures 4(c) and (d) are other SU-8 structures produced with the mask. Au pillars in the masks resulted in holes in SU-8 resist. It is difficult to measure the sidewall roughness of the holes produced with the small gold patterns. However, as the small gold patterns were surrounded by the large gold frame, a large,  $870\ \mu\text{m}$  thick SU-8 square sheet (with holes in the center) was produced when the mask was exposed. The thick SU-8 sheet then allowed atomic force microscopy (AFM) measurement of its roughness. The PBW frame edge (as shown in figure 2) was expected to produce a smooth-sidewall SU-8 structure after the x-ray lithography process. Figure 5(a) shows sidewalls of the  $870\ \mu\text{m}$  thick SU-8 sheet produced by exposure of the frame edges. The arrow in figure 5(a) shows a smooth sidewall that was made by





**Figure 5.** (a) Sidewall of a  $870\ \mu\text{m}$  SU-8 structure fabricated with x-ray lithography through the PBW frame edge (shown by an arrow) and (b) AFM image showing sidewall roughness of the right side in (a). The roughness (rms) is 14.4 nm.

x-ray lithography through the PBW frame edge. The roughness of this sidewall was measured with AFM. Over a scan area of  $5\ \mu\text{m} \times 5\ \mu\text{m}$ , a roughness (rms) of 14 nm was measured (figure 5(b)). Sidewall roughness is an important consideration for many applications, in particular in optics. Moldovan *et al* studied the sidewall roughness of PMMA structures in deep x-ray lithography for several masks, and the roughness was about 25 nm (rms) in the lateral directions [16]. Hall *et al* used masks that were fabricated with e-beam lithography for x-ray lithography and reported somewhat better sidewall roughness (10–14 nm) [17]. Our sidewall roughness of the SU-8 structure is comparable to the roughness reported by Hall *et al*. It should be pointed out that this roughness is not the limit of PBW, because a resist sidewall roughness of around 3 nm was achieved for PBW-written structures. We are currently working on the improvement of this feature of the process.

#### 4. Conclusions

In conclusion, we have manufactured high-quality x-ray masks in a simplified process without intermediate mask copy by using proton beam writing. Mask patterns were transferred by deep x-ray lithography with synchrotron radiation into  $870\ \mu\text{m}$  SU-8 resist with an excellent sidewall quality. Direct proton beam writing combined with electroplating provides a simple and fast way for fabricating x-ray masks with a high quality of the absorber edges.

#### Acknowledgments

The authors acknowledge financial support from the MOE Academic Research Fund under grant R-144-000-130-112 as well as NUS Core Support C-380-003-003-001, A\*STAR/MOE RP 3979908M and A\*STAR 12 105 0038 grants.

#### References

- [1] Becker E W, Ehrfeld W, Hagmann P, Maner A and Muenchmeyer D 1986 Fabrication of microstructures with high aspect ratios and great height by synchrotron radiation lithography, galvanofarming, and plastic moulding (LIGA process) *Microelectron. Eng.* **4** 35–56
- [2] Wang L, Christenson T, Desta Y M, Fetting R K and Goettert J 2004 High-resolution x-ray masks for high aspect ratio microelectromechanical systems applications *J. Microlith., Microfab., Microsyst.* **3** 423–8
- [3] Shan X C, Maeda R, Ikehara T, Mekaru H and Hattori T 2003 Fabrication of X-ray masks and applications for optical switch molding *Sensors Actuators A* **108** 224–9
- [4] Lüttge R, Adam D, Burkhardt F, Hoke F, Schacke H, Schmidt M, Wolf H and Schmidt A 1999 40 keV shaped electron beam lithography for LIGA intermediate mask fabrication *Microelectron. Eng.* **46** 247–50
- [5] Knaack S A, Eddington J, Leonard Q, Cerrina F and Onellion M 2004 Dense arrays of nanopores as x-ray lithography masks *Appl. Phys. Lett.* **84** 3388–90
- [6] van Kan J A, Bettiol A A and Watt F 2006 Proton beam writing of three-dimensional nanostructures in hydrogen silsesquioxane *Nano Lett.* **6** 579–82
- [7] van Kan J A, Bettiol A A and Watt F 2003 Three dimensional nanolithography using proton beam writing *Appl. Phys. Lett.* **83** 1629–31
- [8] Ansari K, van Kan J A, Bettiol A A and Watt F 2004 Fabrication of high aspect ratio 100 nm metallic stamps for nanoimprint lithography using proton beam writing *Appl. Phys. Lett.* **85** 476–8
- [9] Breese M B H, Grime G W and Watt F 1993 MeV ion beam lithography of PMMA *Nucl. Instrum. Methods Phys. Res. B* **77** 169–74
- [10] van Kan J A, Shao P G, Ansary K, Bettiol A A, Osipowicz T and Watt F 2007 Proton beam writing: a tool for high-aspect ratio mask production *Microsyst. Technol.* **13** 431–4
- [11] Watt F, van Kan J A, Rajta I, Bettiol A A, Choo T F, Breese M B H and Osipowicz T 2003 The National University of Singapore high energy ion nano-probe facility: performance tests *Nucl. Instrum. Methods Phys. Res. B* **210** 14–20
- [12] Cheng C M and Chen R H 2001 Development behaviours and microstructure quality of downward-development in deep x-ray lithography *J. Micromech. Microeng.* **11** 692–6
- [13] Moser H O, Jian L K, Casse B D F, Heussler S P, Bahou M, Cholewa M, Kong J R, Saw B T, bin Mahmood S and Yang P 2006 Fabrication and diagnostics of micro/nanodevices by means of synchrotron radiation *J. Phys: Conf. Ser.* **34** 15–21
- [14] van Kan J A, Sum T C, Osipowicz T and Watt F 2000 Sub 100 nm proton beam micromachining: theoretical

- calculations on resolution limits *Nucl. Instrum. Methods Phys. Res. B* **161–163** 366–70
- [15] Meyer P, Schulz J and Hahn L 2003 DoseSim: Microsoft-Windows graphical user interface for using synchrotron x-ray exposure and subsequent development in the LIGA process *Rev. Sci. Instrum.* **74** 1113–9
- [16] Moldovan N, Mancini D C, Divan R, Makarova O V, Peele A and Podolak K R 2002 Side wall roughness in ultradeep x-ray lithography *Microsyst. Technol.* **9** 130–2
- [17] Hall A C, Dugger M T, Prasad S V and Christensen T 2005 Sidewall morphology of electroformed LIGA parts-implications for friction, adhesion, and wear control *J. Microelectromech. Syst.* **14** 326–34